The Reaction between Cyanide and the Hemocyanin of *Carcinus Maenas*. A Kinetic Study

MARIANO BELTRAMINI, FERNANDA RICCHELLI, LAURA TALLANDINI and BENEDETTO SALVATO*

Centro C.N.R. per lo studio della Biochimica e della Fisiologia delle Emocianine e di altre Metallo-proteine. Istituto di Biologia Animale, Università di Padova, Via Loredan 10, 35131 Padua, Italy

Received December 6, 1983

The kinetics of the reaction between Carcinus maenas hemocyanin and cyanide has been studied at various KCN concentrations and at different temperatures (21° and 4 °C) by following the decrease of the copper-peroxide absorption band, centered at 337 nm, of the copper still bound to the protein and the intrinsic fluorescence changes as functions of time. In all conditions used, the absorption band completely disappears and KCN concentration affects only the rate of the process. The reaction is kinetically homogeneous indicating no site–site interaction. The apparent rate constant increases with the square of cyanide concentration and the inverse of O_2 concentration. The copper still bound decreases at a rate slower than the 337 nm absorption and the process is not kinetically homogeneous. The fluorescence of the protein increases after an induction period showing an inflection point at about 50% of the total effect. A kinetic model has been proposed on the assumption that the two metal ions are removed sequentially from the active site. The experimental data are in agreement with the theoretical equations derived from the model. The equilibrium constants for the formation of the complex between the first and the second copper ion with cyanide and the rate constants of their decomposition have been calculated. The rate-limiting process for the removal of the second copper ion is the formation of the complex with cyanide.

Introduction

Hemocyanins (Hcs)‡ are oxygen-carrying multimeric proteins which are found in the hemolymph of several invertebrate species belonging to the Mollusca and Arthropoda [1].

These proteins contain a pair of copper ions at the active site. In the oxygenated state the two metal ions are present as Cu(II) and are antiferromagnetically coupled [2]. The oxygen is bound as peroxide in the ratio 1 O_2^{2-}:2 Cu(II) [3]. In the deoxyform the metal is present as Cu(I). The optical spectral properties of oxy-Hc are rather unusual: the near U.V.–visible spectral region is dominated by a strong band at $\lambda \sim 345$ nm ($\epsilon \sim 20{,}000\ M^{-1}\ cm^{-1}$ per binuclear copper site) and a reasonably intense transition at λ 570 nm ($\epsilon \sim 1{,}000\ M^{-1}\ cm^{-1}$). These spectral features, responsible for the blue colour of oxy-Hc, result from the binding of oxygen to the copper active site and are completely absent in deoxy-, met- and apo-Hc [4].

Cyanide has been known for a long time to cause the decoloration of oxy-Hc and the removal of the metal from the active site. The loss of colour was attributed to the displacement of oxygen which parallels the formation of a complex between copper and cyanide [5]. Subsequently it was demonstrated that cyanide actually extracts the metal from the active site [6]; hence the reaction was reinterpreted as a metal partition between the active site and the external ligand. On this basis Felsenfeld [7] calculated the equilibrium constants for the dissociation of the copper ions. The formation of a Hc–CN^- complex has been inferred also from the modifications of the CD visible spectra, induced by small amounts of cyanide [8].

A further peculiarity of this reaction arises from the kinetic inequivalence of the two copper ions which are sequentially removed: under carefully defined conditions a single copper ion can be selectively displaced and the half-apo Hc is obtained [9, 10]. The experimental evidence for the reaction of CN^- with Hc indicates the occurrence of two distinct processes: the loss of color as the consequence of the formation of a complex Hc–CN and its decomposition which leads to the metal displacement [9].

The study of this reaction can give useful information on the relationship between the two metal ions, and the complex stability, the site accessibility, the conformational modifications of the protein and the cooperative interaction within the quaternary structure.

‡Abbreviations used: CD: Circular dichroism. Hc: Hemocyanin.

*To whom correspondence and requests for reprints should be addressed.

0020-1693/84/$3.00

According to their peculiar properties at the level of quaternary structure, Hcs can be divided into three classes: molluscan Hc, crustacean Hc and the Hc of Arachnomorpha [11]. A detailed study of the reaction with cyanide has been undertaken in our laboratory using *Octopus vulgaris*, *Carcinus maenas* and *Limulus polyphemus* as representative species of the above-mentioned groups. In this paper the results obtained with *Carcinus maenas* Hc are reported. The dependence of the reaction rate *vs.* cyanide concentration, oxygen partial pressure and temperature has been studied following the absorbance of the copper–peroxide band at 337 nm, the protein fluorescence and the copper still bound to the protein, as functions of time.

Experimental

Materials and Methods

Fresh hemolymph was collected with a syringe from the dorsal lacuna of living animals, filtered on gauze and centrifuged at 3000 r.p.m. The clear supernatant was diluted 1:1 with Tris/HCl pH = 7.2, $\mu = 0.1$ containing $CaCl_2$ 20 m*M*. Solid $(NH_4)_2\ SO_4$ was added up to a final saturation of 52%. After 1–2 hours, the bluish suspension was centrifuged at 15000 r.p.m., the pellet was redissolved in the same buffer and reprecipitated as above.

The protein solution (60–80 mg/ml) was dialyzed against Tris/HCl buffer for 48 hours; sucrose (18% w/v) was added and the final protein solution was stored at −20 °C. Alternatively, the protein was prepared by double sedimentation in the Spinco-Beckman Mod. L 50 preparative ultracentrifuge at 60000 r.p.m. for 5 hours. All operations were carried out at 4 °C.

Chemicals were of analytical grade and were used without further purification.

Protein concentration was determined spectrophotometrically using the values $E_{288}^{0.1\%} = 1.41$ in 0.5 *M* NaOH and $E_{278}^{0.1\%} = 1.24$ in Tris/HCl $\mu = 0.1$, pH 8.0. The absorbances were corrected for light scattering as described elsewhere [12].

Optical spectra were taken with a Perkin-Elmer Mod. 402 spectrophotometer equipped with a repetitive scanning device and thermostatted cell compartment.

Fluorescence spectra were recorded with a MPF 4 Perkin-Elmer spectrofluorimeter equipped with a thermostatted cell compartment. Copper was estimated by atomic absorption, using a Perkin-Elmer 300 spectrophotometer.

Solutions containing 4–5 mg/ml of protein in Tris/HCl buffer pH 8.0, $\mu = 0.1$ plus 20 m*M* $CaCl_2$ were used for kinetic measurements. Two series of experiments were carried out, at 4° ± 0.1 °C and 21 ± 0.1 °C respectively. The solutions were prepared with thermostatted buffer equilibrated with air moistened by bubbling through two wash-bottles containing the same buffer at the same temperature.

To 5 ml of protein solution, different amounts (50–500 μl) of freshly prepared 0.25 *M* KCN in the same buffer were added. A portion of the reaction mixture was used for repetitive automatic recording of the absorption spectra between 300 and 390 nm. The remaining part was employed for the measurement of the copper still bound and of the fluorescence. For copper determinations, 200 μl aliquots of the reaction mixture, collected at different times, were diluted in 2 ml of buffer; after 48 hr of dialysis against the same buffer in the cold, the ratio Cu/Hc was measured. Preliminary experiments with both apo and native protein solutions containing different amounts of added Cu^+ and CN^- indicated that, under these conditions, dissociated copper is completely eliminated.

Fluorescence spectra were taken at different times on samples obtained by diluting 20 μl of the reaction mixture in 3 ml of buffer. The absorbance of these solutions at the excitation wavelength (280 nm) was about 0.03 to avoid corrections due to the inner filter effects. The spectra were monitored in the ratio mode to minimize the errors arising from lamp fluctuations.

Kinetic experiments at different pO_2 were done using a rubber septum-stoppered tonometer of 70 ml total volume provided with a quartz cuvette of 1 cm light path. To the Hc solution equilibrated at the desired O_2 pressure, a measured volume of 0.25 *M* KCN solution was injected through the septum. These experiments were carried out at 21° ± 0.1 °C and at a final KCN concentration of 7.11×10^{-3} *M*. The determination of the equilibrium constants of Hc with $O_2(K_{O_2})$ was made using a tonometric method [13].

Results and Discussion

At concentrations lower than 1×10^{-4} *M*, cyanide does not affect the spectral properties of native *Carcinus* Hc. At higher concentrations, a time-dependent decrease of the absorbance at 337 nm is observed. In all cases, the absorption band completely disappears, and the cyanide concentration affects only the rate of the process (Fig. 1A). As cyanide was in large excess over Hc in all experiments, its concentration can be considered time-independent.

In Fig. 1(A, B), the results of a typical experiment at 21 °C are shown. The semilogarithmic plot of ln A_0/A_t *vs.* time gives a straight line intersecting the origin. In all kinetic experiments the absorbance values were corrected for the absorbance, A_∞, at the end of the reaction to correct for the residual protein absorption.

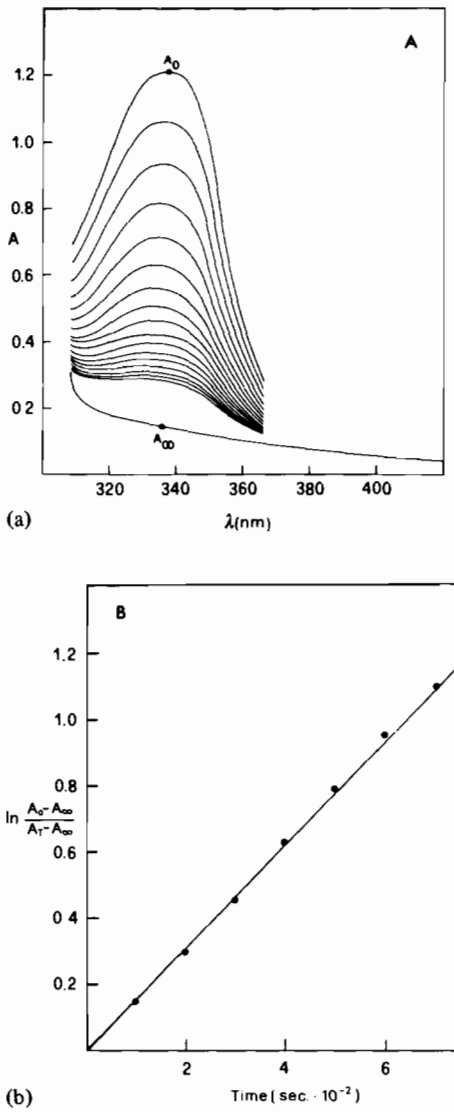

Fig. 1. (A) Automatic recording of the copper–peroxide absorption band (310–365 nm) during the reaction of *Carcinus maenas* hemocyanin (5 mg/ml) and cyanide (24 m*M*) at T = 4 °C, Δt = 100 sec. A_0 and A_∞ indicate the absorbances at 337 nm recorded at time zero and at the end of reaction. (B) Semilogarithmic plot of the absorbance at 337 nm *vs.* time using the data from (A).

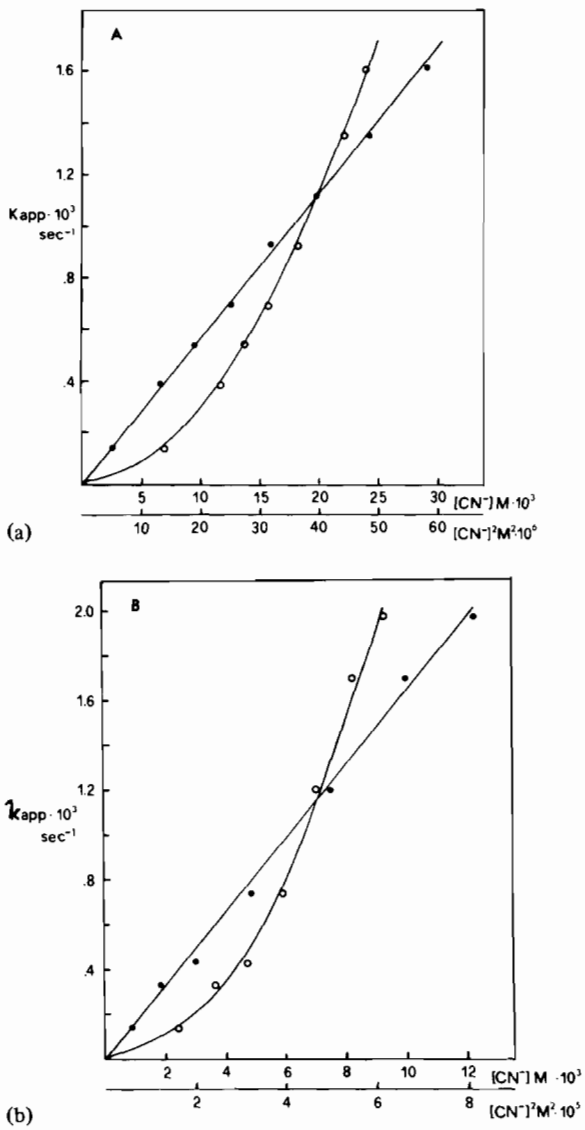

Fig. 2. Dependence of k_{app} from cyanide concentration (○) and from the square of cyanide concentration (●). (A) Data obtained at 4 °C. (B) Data obtained at 21 °C. Protein concentration ~5 mg/ml in Tris/HCl pH 8.0 μ = 0.1

The slope (k_{app}) increases with increasing KCN concentration both at 4° and 21 °C following a parabolic trend (Fig. 2A, B). In fact, a straight line is obtained when the data are plotted *vs.* the square of cyanide concentration. The comparison of the data obtained at the two different temperatures discloses a large temperature dependence of the reaction rate.

The effect of cyanide on the optical spectrum of Hc is strongly depressed by increasing the O_2 concentration: the plot of the observed pseudo-first order rate constants (k_{app}) *versus* the O_2 concentration shows an hyperbolic trend (Fig. 3): a straight line is obtained when the reciprocal of O_2 concentration is reported in the abscissa (Fig. 3).

In all experimental conditions the decrease of the absorbance at 337 nm can be described by a single exponential. The time dependence of the copper still bound, however, shows differences according to the temperature of the experiment.

In Fig. 4 are reported plots of the dependency of A_{337}, the absorbance at 337 nm (A, D), the copper still bound to the protein (B, E) and the increase of protein fluorescence (C, F) against the time of reaction with cyanide at 4 °C (A, B, C) and 21 °C (D, E, F). The values of A_{337} and the copper still bound

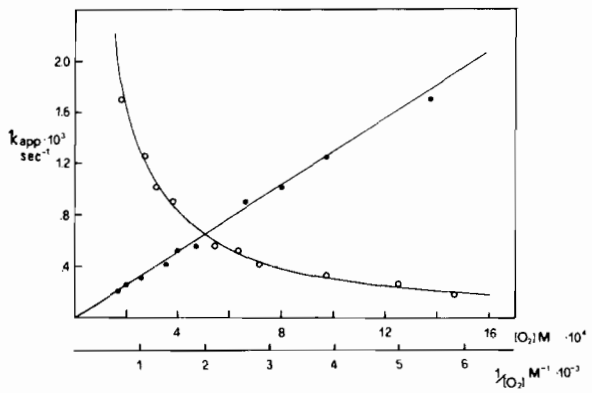

Fig. 3. Dependence of k_{app} from O_2 concentration (○) and from $1/O_2$ concentration (●); $T = 21$ °C; 7.11 m*M* KCN. Protein concentration ~5 mg/ml in Tris/HCl pH 8.0 $\mu = 0.1$.

measured during the reaction are reported as a percentage of the corresponding values in the native protein. The changes in the fluorescence emission intensity (F) at $\lambda_{em} = 345$ nm ($\lambda_{exc} = 280$ nm) of Hc are reported as F/F_0 where F_0 is the fluorescence measured in the absence of CN^-.

At 4 °C the amount of copper still bound decreases more slowly than the absorbance at each KCN concentration; furthermore the process cannot be described by a single exponential. At 21 °C a biphasic trend is evident especially at low cyanide concentrations. Copper is removed in two sequentially linked steps each involving 50% of the total metal content. The first step approximately follows the absorbance decrease. In the second step, after an induction time, the rate suddenly increases up to the value of the first one. The increase of KCN concentration reduces the difference in the rates of the processes involving the absorption band and the copper release. This occurs at both temperatures.

The trends of the F/F_0 ratio *vs.* time are quite similar at 4 °C and 21 °C. An induction time is observed especially at 4 °C and at low KCN concentrations; moreover an inflection region appears which is more evident at 21 °C. Upon increasing the KCN concentration the curves become smoother and the induction time shortens. The limiting value of the F/F_0 ratio is about 5.

Native *Carcinus maenas* Hc exists in the hemolymph as large aggregates having a characteristic

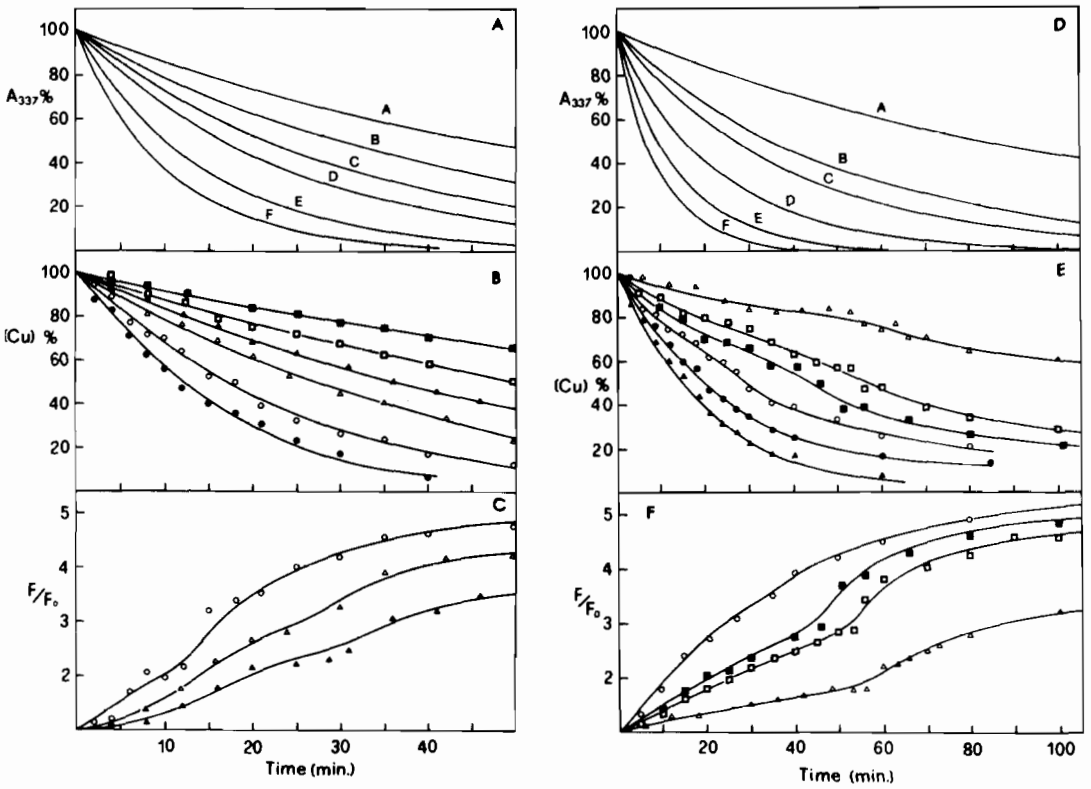

Fig. 4. Time dependence of the absorbance at 337 nm (A, D), of copper still bound (B, E) and F/F_0 ratio (C, F) at 4 °C (A, B, C) and 21 °C (D, E, F). Letters and symbols refer to different KCN concentrations: at 4 °C (A, ■), 9.15 m*M*; (B, □), 11.5 m*M*; (C, ▲), 13.7 m*M*; (D, △), 15.8 m*M*; (E, ○), 20.0 m*M*; (F, ●), 23.4 m*M*; at 21 °C: (A, △), 2.4 m*M*; (B, □), 3.56 m*M*; (C, ■), 4.75 m*M*; (D, ○), 5.88 m*M*; (E, ●), 7.05 m*M*; (F, ▲), 8.16 m*M*. Buffer: Tris/HCl pH 8.0 $\mu = 0.1$.

structure and sedimentation coefficients of 24S and 16S. These aggregates are stable up to pH 10. The removal of copper does not induce dissociation. When native Hc is compared with apo-Hc, only minor structural differences are observed [14].

The reaction with cyanide must be considered reversible because the native protein can be reconstituted from apo-Hc by adding several Cu(I) complexes including K_3 $Cu(CN)_4$ [9, 15]. In spite of the multimeric nature of this Hc, the absorption change upon cyanide addition is an homogeneous process indicating the absence of cooperative phenomena between the subunits. However, at 21 °C some cooperativity can be seen especially at low KCN concentrations. The biphasic trend of the curves describing the copper still bound (Fig. 4B, E), clearly shows that the metal ions are removed sequentially from the active site. The final product of the CN^- reaction is apo-Hc regardless of the concentration of ligand used. This observation rules out the possibility that the reaction may consist of a simple distribution of the metal between the protein active site and the external ligand. In proposing a model for this reaction all the above-mentioned considerations together with the observed dependence of the reaction rates *vs.* KCN and O_2 concentrations must be taken into account. Cyanide affects *Carcinus maenas* Hc in at least two steps which are sequentially linked: (1) the formation of the complex HcCN which is measured by the decrease of the copper–peroxide absorption band; (2) the decomposition of the complex with the involvement of a second CN^- ion.

The asymmetry between the data concerning the absorption band and the protein-bound copper requires that both steps occur for each metal ion sequentially in the active site. The experimental data are interpreted on the basis of the following reaction model:

$$Hc + O_2 \overset{K_{O_2}}{\rightleftharpoons} HcO_2 \qquad (A)$$

$$Hc + CN^- \overset{K_{CN}}{\rightleftharpoons} HcCN \qquad (B)$$

$$HcCN + CN^- \xrightarrow{k_1} Hc^\circ + [Cu(CN)_2]^- \qquad (C)$$

$$Hc^\circ + CN^- \overset{K^\circ_{CN}}{\rightleftharpoons} Hc^\circ CN \qquad (D)$$

$$Hc^\circ CN + CN^- \xrightarrow{k_2} Hc^{\circ\circ} + [Cu(CN)_2]^- \qquad (E)$$

where $Hc^{\circ\circ}$ is the copper-free protein and Hc° is the protein containing a single copper ion in the active site. In this model the removal of copper occurs stepwise with previous formation of a complex between the copper bound to the protein and the ligand (HcCN, $Hc^\circ CN$). The equations (C) and (E) should be considered as equilibria; under our experimental conditions, however, the reverse reactions are unlikely to occur.

The mathematical treatment of the model (see the Appendix) has assumed that: (1) the equilibria (A, B, D) which involve oxygen and cyanide are very fast compared with the other reactions (C, E); (2) the concentration of free Hc is very low and can be considered time-independent; and (3) the concentrations of cyanide and oxygen are large enough with respect to the Hc, hence they can be considered constant during the reaction time, and the equations C and E take the form of pseudo first-order kinetics.

The equilibrium constants K_{O_2}, K_{CN} and K°_{CN} for the equations A, B and D are dissociation constants.

According to the model proposed (see Appendix) the decrease in the 337 nm absorbance which is a measure of the concentration of oxy-Hc can be described by a single exponential:

$$A_t = A_0 \, e^{-k_{app}t} \qquad (1)$$

where A_0 and A_t are the absorbances at 337 nm measured at the beginning and during the reaction with CN^- and k_{app} is the apparent rate constant of the process.

The analytical expression of k_{app} is given in the following equation:

$$k_{app} = k_1 \frac{K_{O_2}[CN^-]^2}{K_{O_2}[CN^-] + K_{CN}[O_2]} \qquad (2)$$

A simplified form of eqn. (2) can be used, however, because under our conditions the value of $K_{O_2}[CN^-]$ is lower than 5% of the value $K_{CN}[O_2]$:

$$k_{app} = k_1 \frac{K_{O_2}[CN^-]^2}{K_{CN}[O_2]} \qquad (2')$$

This simplification is in good agreement with our experimental data, within the experimental error: according to eqn. (2'), k_{app} depends solely on the square of $[CN^-]$ (Fig. 2A, B) and the inverse of $[O_2]$ (Fig. 3). For a better evaluation of the kinetic data we used a rearrangement of the analytical form of k_{app} (eqn. (2)) which allows the calculation of the separate values of k_1 and K_{O_2}/K_{CN}:

$$\frac{[CN^-]}{k_{app}} = \frac{1}{k_1} + \frac{1}{k_1}\frac{K_{CN}}{K_{O_2}}\frac{[O_2]}{[CN^-]} \qquad (3)$$

Thus, the plot of $[CN^-]/k_{app}$ against $1/[CN^-]$ at constant $[O_2]$ or against $[O_2]/[CN^-]$ is a straight line with intercept $1/k_1$ and slope $(1/k_1)(K_{CN}/K_{O_2})$. The experimental values of $[CN^-]/k_{app}$ (from the data of Fig. 2A) *versus* $1/[CN^-]$ obtained at 4 °C and that of $[CN^-]/k_{app}$ *versus* $[O_2]/CN^-$ at 21 °C (from the data of Fig. 2B and 3) are shown in Fig. 5A and B respectively.

In both cases the least-squares evaluation of the experimental data gives straight lines which do not pass through the origin and have a very high correla-

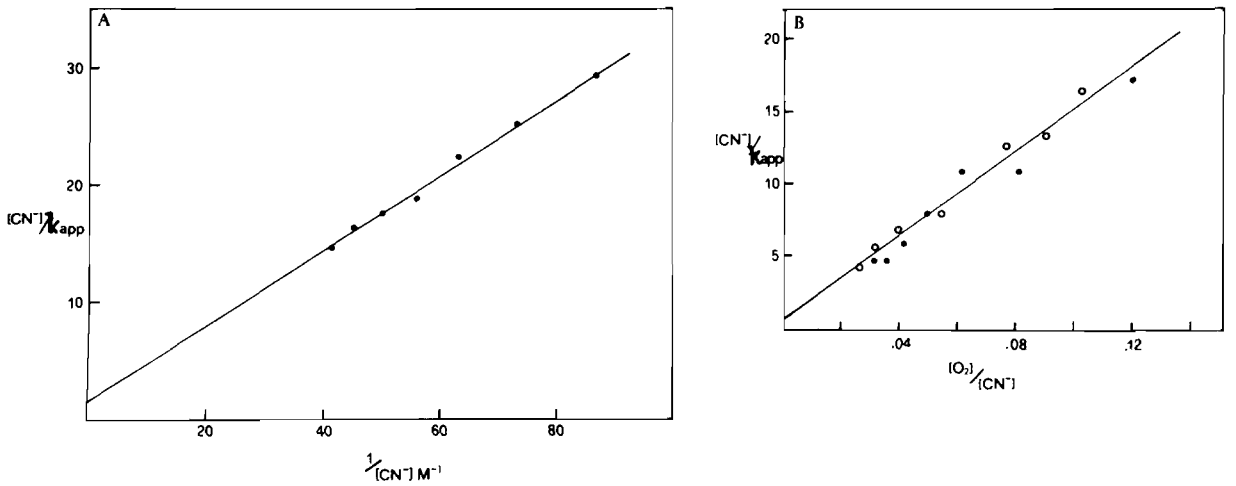

Fig. 5. A: Dependence of $[CN^-]/k_{app}$ on $1/[CN^-]$ at 4 °C. The data are obtained at O_2 concentration = 0.4 mM. B: Dependence of $[CN^-]/k_{app}$ on $[O_2]/[CN^-]$ at 21 °C. (•) 0.28 mM O_2 concentration; (○) 7.11 mM cyanide concentration.

tion coefficient ($r > 0.9$). In Table I the values for k_1 and the K_{CN}/K_{O_2} ratio at both temperatures are reported. The values of K_{CN} were calculated using the experimental values of K_{O_2} also reported in Table I.

From the values of k_1 measured at the two different temperatures it is possible to calculate the activation energy of the process. The activation energy of the reaction involving the displacement of the first copper ion is equal to 6,300 cal/mol. The enthalpy variation, $\Delta H_{K_{CN}}$ of the equilibrium reaction of Hc with cyanide has a negative value of −12,000 cal/mol. This implies that an increase in temperature favours the formation of the complex HcCN, perhaps owing to an increased accessibility of the metal ion. However, this explanation may rationalize only part of the temperature effect if we consider the large negative value of the $\Delta H_{K_{CN}}$. Alternatively, the formation of the complex HcCN could involve the loss of one or more metal–protein bonds. In this case, $\Delta H_{K_{CN}}$ contains one negative term relative to the breakage of metal protein ligand bonds and one positive term arising from the formation of the metal–CN bond. At present, no further information is available to support either of these explanations.

The model gives separate equations for the displacement of the first and second copper ion from the active site. The following equation describes the total metal displacement:

$$[Cu]_t = [HcO_2]_0 \left(\frac{2k_0 - k_{app}}{k_0 - k_{app}} e^{-k_{app} t} - \frac{k_{app}}{k_0 - k_{app}} e^{-k_0 t} \right) \quad (4)$$

where $[Cu]_t$ is the concentration of the copper still bound to the protein at time t, $[HcO_2]_0$ the concentration of oxy-hemocyanin at the beginning of the reaction and k_0 is a function of the rate constant k_2, of the equilibrium dissociation constant K°_{CN} relative to the second copper ion and of CN^- concentration according to the equation:

$$k_0 = \frac{k_2 [CN^-]^2}{[CN^-] + K^\circ_{CN}} \quad (5)$$

The interpolation curves of Fig. 4B, E are calculated according to eqn. 4 using the experimental values of k_{app} and the k_0 values which give the best fit with the experimental data, using a non-linear least-squares treatment of the data.

TABLE I. Kinetic and Thermodynamic Data of the Reaction between *Carcinus maenas* Hemocyanin and Cyanide according to the Proposed Model.

T (°C)	k_1 (M^{-1} s^{-1})	k_2 (M^{-1} s^{-1})	K_{CN}/K_{O_2}	K_{O_2} (M)	K_{CN} (M)	K°_{CN} (M)	$(E_{ATT})_{k_1}$ (cal/mol)	$(\Delta H)_{K_{O_2}}$ (cal/mol)	$(\Delta H)_{K_{CN}}$ (cal/mol)
4	0.803	0.68	625.25	1.09×10^{-6}	7.15×10^{-4}	0.24	6300	−1800	−12000
21	1.560	–	225.43	0.90×10^{-6}	2.03×10^{-4}	–			

Equation 5 can be rearranged as eqn. 3, thus allowing the calculation of separate values for k_2 and K°_{CN} (Fig. 6):

$$\frac{[CN^-]}{k_0} = \frac{1}{k_2} + \frac{K^\circ_{CN}}{k_2}\,\frac{1}{[CN^-]} \qquad (6)$$

The results are summarized in Table I.

At 4 °C, k_2 is 0.68 M^{-1} sec^{-1}, close to the value of k_1, indicating that the two copper ions are removed from the complexes HcCN or Hc°CN with the same efficiency. K°_{CN}/k_2 has a value of 0.36 M^2 sec and K°_{CN} of 0.24 M. The value K°_{CN} relative to the reaction of CN^- to the half-apoHc (Hc°) is more than two orders of magntude higher than the corresponding value of the equilibrium constant ($K_{CN} = 7.5 \times 10^{-4}$ M) for cyanide binding to the first copper ion.

Thus, the formation of the complex Hc°CN is the rate limiting step for the displacement of the second copper ion. This observation can be explained assuming that the removal of the first Cu ion induces a conformational change which reduces the accessibility of CN^- to the second metal ion still bound to the protein.

This interpretation is supported by the fluorescence data. The fluorescence emission intensity increases on going from oxy- to apoHc [16]. This effect is the consequence of peroxide and copper removal from the active site which are capable of quenching the emission of the protein *via* an energy-transfer [16] or a heavy metal effect [17], respectively. The ratio F_{apo}/F_{oxy} is about 5. The presence of the induction period and of the inflection region supports the occurrence of a conformational rearrangement depending on the removal of both copper ions. It also shows that, at a molecular level, the complexity of the reaction is greater than that suggested by the kinetic data only. As pointed out before, the comparison of the CD spectra of native and epo-Hc shows that the removal of copper induces only minor conformational changes [14]. As a consequence, the structural modification responsible for the differences in K_{CN} and K°_{CN} is expected to be small and restricted within the region of the active site.

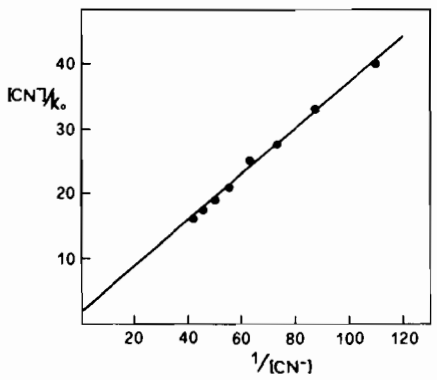

Fig. 6. Dependence of $[CN^-]/k_0$ from $1/[CN^-]$. Conditions as in Fig. 5A.

The model does not adequately describe all the data obtained at 21 °C. Probably, at low KCN concentrations, the quaternary structure mediates cooperative effects, leading to a separation between the processes involving the two copper ions.

The structure of the Hc active site has been widely investigated. Histidine (2–4 per copper ion) and probably 1 tyrosine have been proposed as metal ligands [3, 12, 18, 19]. The model proposed for the active site of oxy-Hc consists of a structure in which each Cu(II) ion is linked by 2 or 3 histidines and a water molecule; the two metal centres which are 3.67 Å apart are further connected by an inner bridging ligand (probably a phenolate) [4, 20]. The data here reported on *Carcinus* Hc and those obtained for other Hc species [9] as well as the possibility of preparing half-apo forms from both arthropod [21] and molluscan Hc make evident, at least kinetically, the inequivalence of the two metal ions. The apparent discrepancy between these findings and the active site model could imply an asymmetric localization of the two metal centers shielded within the protein matrix, which exerts a fine control on the site accessibility.

Recent studies [22] concerning the correlation between the copper content and the intrinsic fluorescence of *Carcinus maenas* Hc show that the fluorescence quenching is due only to the fast-removed copper ion. The lack of a linear correlation, here reported, between the removal of metal and the fluorescence changes implies that these changes also involve a conformational rearrangement in the region of the binding site and probably the transfer of the slow-reacting copper to the free site of the fast-reacting one.

Acknowledgements

We are greatly indebted to Dr. Jack Peisach and Dr. William Blumberg for critical discussion.

References

1 M. Brunori, B. Giardina and J. V. Bannister, in 'Inorganic Biochemistry', (Hill, H.A.O., Ed.), Vol. 1, p. 159, Chemical Society, London (1980).
2 E. I. Solomon, D. M. Dooley, R. H. Wang, H. B. Gray, M. Cerdonio, F. Mogno and G. L. Romani, *J. Am. Chem. Soc., 98,* 1029 (1976).
3 J. S. Loehr, T. B. Freedman and T. M. Loehr, *Biochem. Biophys. Res. Commun., 56,* 510 (1974).
4 N. C. Eickman, R. S. Himmelwright and E. I. Solomon, *Proc. Natl. Acad. Sci. U.S.A., 76,* 2094 (1979).
5 O. H. Pearson, *J. Biol. Chem., 115,* 171 (1936).
6 F. Kubowitz, *Biochem. Z., 299,* 32 (1938).
7 G. Felsenfeld, *J. Cell. Comp. Physiol., 43,* 23 (1954).

8 M. De Ley and R. Lontie, *Biochim. Biophys. Acta, 278,* 404 (1972).
9 B. Salvato and P. Zatta, in 'Structure and Function of Hemocyanin', (Bannister, J.V., Ed.), p. 245, Springer-Verlag, Berlin (1977).
10 R. S. Himmelwright, N. C. Eickman, C. D. Lu Bien and E. I. Solomon, *J. Am. Chem. Soc., 102,* 5378 (1980).
11 A. Ghiretti-Magaldi and G. Tamino, in 'Structure and Function of Hemocyanin', (Bannister, J.V., Ed.), p. 271, Springer-Verlag, Berlin (1977).
12 B. Salvato, A. Ghiretti-Magaldi and F. Ghiretti, *Biochemistry, 13,* 4778 (1974).
13 A. F. Riggs and R. A. Wolbach, *J. Gen. Physiol., 39,* 585 (1956).
14 A. M. Tamburro, B. Salvato and P. Zatta, *Comp. Biochem. Physiol. (part. B), 55,* 347 (1976).
15 M. Beltramini and K. Lerch, in 'Structure and Function of Invertebrate Respiratory Proteins', (Wood, E. J., Ed.) in 'Life Chemistry Reports', Sup. 1, p. 323, Harwood Academic, London (1983).
16 N. Shaklai and E. Daniel, *Biochemistry, 9,* 564 (1970).
17 W. H. Bannister and E. J. Wood, *Comp. Biochem. Physiol., 40B,* 7 (1971).
18 G. Jori, S. Cannistraro, F. Ricchelli, B. Salvato and L. Tallandini, in 'Invertebrate Oxygen-Binding Proteins', (Lamy, J. & Lamy, J., Eds.), p. 621, Marcel Dekker, New York (1981).
19 E. I. Solomon, in 'Copper Proteins', (Spiro, T. G., Ed.), Vol. 3, p. 41, Wiley–Interscience, New York (1981).
20 J. M. Brown, L. Powers, B. Kincaid, J. A. Larrabee and T. B. Spiro, *J. Am. Chem. Soc., 102,* 4210 (1980).
21 B. Salvato, in preparation.
22 F. Ricchelli, E. Tealdo and B. Salvato, in 'Structure and Function of Invertebrate Respiratory Proteins', (Wood, E.J., Ed.), in 'Life Chemistry Reports', Sup. 1, p. 301, Harwood Academic, London (1983).

Appendix

The model:

$$Hc + O_2 \overset{K_{O_2}}{\rightleftharpoons} HcO_2$$

$$Hc + CN^- \overset{K_{CN}}{\rightleftharpoons} HcCN$$

$$HcCN + CN^- \xrightarrow{k_1} Hc^\circ + [Cu(CN)_2]^-$$

$$Hc^\circ + CN^- \overset{K^\circ_{CN}}{\rightleftharpoons} Hc^\circ CN$$

$$Hc^\circ CN + CN^- \xrightarrow{k_2} Hc^{\circ\circ} + [Cu(CN)_2]^-$$

is described by the following system of differential equations:

$$\frac{d[HcO_2]}{dt} = k^1_{O_2}[Hc][O_2] - k^{-1}_{O_2}[HcO_2] \quad (1)$$

$$\frac{d[Hc]}{dt} = k^{-1}_{O_2}[HcO_2] + k^{-1}_{CN}[HcCN] - k^1_{O_2}[Hc][O_2] - k^1_{CN}[Hc][CN^-] \quad (2)$$

$$\frac{d[HcCN]}{dt} = k^1_{CN}[Hc][CN^-] - k^{-1}_{CN}[HcCN] - k_1[HcCN][CN^-] \quad (3)$$

$$\frac{d[Hc^\circ]}{dt} = k_1[HcCN][CN^-] - k^{\circ 1}_{CN}[Hc^\circ][CN^-] + k^{\circ -1}_{CN}[Hc^\circ CN] \quad (4)$$

$$\frac{d[Hc^\circ CN]}{dt} = k^{\circ 1}_{CN}[Hc^\circ][CN^-] - k^{\circ -1}_{CN}[Hc^\circ CN] - k_2[Hc^\circ CN][CN^-] \quad (5)$$

$$\frac{d[Hc^{\circ\circ}]}{dt} = k_2[Hc^\circ CN][CN^-] \quad (6)$$

The system must be considered together with the mass equation and the zero and infinite time conditions;

$$[Hc]_{tot} = [HcO_2] + [Hc] + [HcCN] + [Hc^\circ] + [Hc^\circ CN] + [Hc^{\circ\circ}] \quad (7)$$

$$[Hc]_{tot} = [HcO_2]_0 = [Hc^{\circ\circ}]_\infty \quad (8)$$

In eqn. (7) [Hc] may be supposed to be very low and in a steady state.

Taking into account the sum of eqns. (4), (5), (6), and making the derivative of eqn. (7) with respect to time, eqn. (9) is obtained:

$$\frac{d[HcO_2]}{dt} + \frac{d[HcCN]}{dt} + k_1[HcCN][CN^-] = 0 \quad (9)$$

Assuming that the equilibria of Hc with O_2 and CN^- are very rapid with respect to the other reactions, and $d[Hc]/dt \sim 0$, from eqn. 2 we obtain:

$$[HcCN] = \frac{K_{O_2}}{K_{CN}} \frac{[CN^-]}{[O_2]} [HcO_2] \quad (10)$$

The derivative with respect to time of eqn. (10) gives:

$$\frac{d[HcCN]}{dt} = \frac{K_{O_2}}{K_{CN}} \frac{[CN^-]}{[O_2]} \frac{d[HcO_2]}{dt} \quad (11)$$

The combination of eqns. (9) and (11) gives:

$$\frac{d[HcO_2]}{dt}\left(\frac{K_{O_2}}{K_{CN}} \frac{[CN^-]}{[O_2]} + 1\right) = -k_1 \frac{K_{O_2}}{K_{CN}} \frac{[CN^-]^2}{[O_2]} [HcO_2] \quad (12)$$

the integration of which between 0 and t time, gives:

$$\ln \frac{[HcO_2]_0}{[HcO_2]_t} = k_1 \frac{K_{O_2}[CN^-]^2}{K_{O_2}[CN^-] + K_{CN}[O_2]} t \quad (13)$$

This equation describes the time dependence of the 337 nm absorption band at given CN^- and O_2 concentrations.

According to our experimental data, this equation may be simplified as follows:

$$\ln \frac{[HcO_2]_0}{[HcO_2]_t} = k_1 \frac{K_{O_2}}{K_{CN}} \frac{[CN^-]^2}{[O_2]} t \qquad (14)$$

Thus the time dependence of the 337 nm absorption band is described by a single exponential, the rate constant value depending on the square of CN^- concentration and on the inverse of O_2 concentration.

The angular coefficient k_{app} of eqn. (13), rearranged, allows the calculation of the separate values of k_1 and K_{O_2}/K_{CN}

$$\frac{[CN^-]}{k_{app}} = \frac{1}{k_1} + \frac{K_{CN}}{K_{O_2}} \frac{[O_2]}{k_1} \frac{1}{[CN^-]} \qquad (15)$$

According to the model, the displacement of the first copper ion follows the same kinetics as the 337 nm absorption band, so that:

$$[Cu]^\circ_t = [Cu]^\circ_0 \, e^{-k_{app} t} \qquad (16)$$

$$k_{app} = k_1 \frac{K_{O_2}}{K_{CN}} \frac{[CN^-]^2}{[O_2]} \qquad (16')$$

As for the second copper ion, the derivation of the equation

$$K^\circ_{CN} = \frac{[Hc^\circ][CN^-]}{[Hc^\circ CN]} \qquad (17)$$

gives:

$$\frac{d[Hc^\circ]}{dt} = \frac{K^\circ_{CN}}{[CN^-]} \frac{d[Hc^\circ CN]}{dt} \qquad (18)$$

Furthermore the sum of eqns. (4) and (5) gives:

$$\frac{d[Hc^\circ]}{dt} + \frac{d[Hc^\circ CN]}{dt} = k_1[HcCN][CN^-] - k_2[Hc^\circ CN][CN^-] \qquad (19)$$

The combination of (18) and (19) gives:

$$\frac{d[Hc^\circ CN]}{dt} = \frac{k_1[HcCN][CN^-]^2}{K^\circ_{CN} + [CN^-]} - \frac{k_2[CN^-]^2}{K^\circ_{CN} + [CN^-]} [Hc^\circ CN] \qquad (20)$$

Substituting for [HcCN] the result of the combined eqns. (10) and (14) and taking

$$\frac{k_2[CN^-]^2}{K^\circ_{CN} + [CN^-]} = k_0 \qquad (21)$$

the following linear differential equation of the first order is obtained:

$$\frac{d[Hc^\circ CN]}{dt} = [Hc]_{tot} \frac{k_{app} k_0}{k_2 [CN^-]} e^{-k_{app} t} - k_0 [Hc^\circ CN] \qquad (22)$$

By integration we obtain:

$$[Hc^\circ CN] = \frac{k_{app} k_0}{(K_0 - k_{app}) k_2 [CN^-]} [Hc]_{tot} \times (e^{-k_{app} t} - e^{-k_0 t}) \qquad (23)$$

By substituting expression (23) for $[Hc^\circ CN]$ in eqn. (6) and by integrating we obtain:

$$[Hc^{\circ\circ}] = [Hc]_{tot} \times \left(- \frac{k_0}{k_0 - k_{app}} e^{-k_{app} t} + \frac{k_{app}}{k_0 - k_{app}} \times e^{-k_0 t} + 1 \right) \qquad (24)$$

From eqn. 7 and the mass equation for the second copper:

$$[Cu]^{\circ\circ} = [HcO_2] + [Hc] + [HcCN] + [Hc^\circ] + [Hc^\circ CN]$$

the second copper still bound results:

$$[Cu]^{\circ\circ} = [Hc]_{tot} - [Hc^{\circ\circ}]$$

which combined with eqn. 24 gives:

$$[Cu]^{\circ\circ}_t = [Hc]_{tot} \times \left(\frac{k_0}{k_0 - k_{app}} e^{-k_{app} t} - \frac{k_0}{k_0 - k_{app}} e^{-k_0 t} \right) \qquad (25)$$

The sum of eqns. (16) and (25) gives the total Cu still bound at any time:

$$[Cu]_t = [Hc]_{tot} \times \left(\frac{2k_0 - k_{app}}{k_0 - k_{app}} e^{-k_{app} t} - \frac{k_{app}}{k_0 - k_{app}} e^{-k_0 t} \right) \qquad (26)$$

The expression 21, rearranged as follows, allows the calculation of the separate values of k_2 and K°_{CN}.

$$\frac{[CN^-]}{k_0} = \frac{1}{k_2} + \frac{K^\circ_{CN}}{k_2} \frac{1}{[CN^-]}$$